

Novel Information about Vibrational Relaxation in Liquids Using Time-Resolved Stokes Probing after Picosecond IR Excitation

G. Seifert,* R. Ziirl, and H. Graener

Martin-Luther-Universität Halle-Wittenberg, Fachbereich Physik, D-06099 Halle, Germany

Received: July 13, 1999; In Final Form: October 13, 1999

The use of Stokes difference spectra for picosecond studies of vibrational relaxation dynamics in condensed matter is introduced and compared to the established techniques of measuring anti-Stokes scattering or IR transmission changes. A simple quantum mechanical description reveals the principal similarities and differences of the different probing processes for the case of moderately anharmonic oscillators, e.g., liquids with only relatively weak interactions of the sample molecules. The outcome is illustrated by novel experiments on neat liquid chloroform, whose relaxation is known quite well. It is shown that transient Stokes data allow additional information, particularly about the behavior of low-lying vibrational levels and the type of energy transfer during relaxation, to be obtained.

Introduction

The study of vibrational population relaxation processes has become a widely used tool to investigate ultrafast dynamical properties of condensed matter. Experiments allowing direct time-resolved observations typically apply intense ultrashort laser pulses for the excitation process. To create a significant amount of excess population on a certain vibrational state, either resonant IR absorption^{1–4} or stimulated Raman scattering¹ can be used. The desired information about the population dynamics requires monitoring of the time evolution of the created population at the best of all vibrational modes. Often population relaxation is used as a probe for further properties such as orientational motion,⁵ hydrogen bond dynamics,⁶ or structural relaxation.⁷ For molecules in the gas phase, IR fluorescence is well suited for this purpose.⁸ In condensed matter fluorescence becomes negligible due to far more efficient nonradiative processes; other probing techniques such as spontaneous anti-Stokes scattering or detection of the induced IR transmission changes (e.g., IR double resonance) have to be used. It has been demonstrated previously that, as a consequence of different selection rules of Raman and IR probing, in most cases a combination of both techniques⁹ is necessary to get a really comprehensive insight into the relaxation phenomena. In this paper, it will be shown that transient Stokes difference spectra can provide additional information, because they combine the easy Raman access to low-frequency vibrations with the possibility to directly observe ground state recovery. These features are first discussed theoretically with the help of a simple quantum mechanical description of the different experimental approaches and then demonstrated presenting novel experimental results on the well-known system of neat liquid chloroform.

Theoretical Considerations

The interaction between a light field and a molecular vibration is treated quantum mechanically starting with a Hamiltonian accounting for both infrared and Raman-type interactions. The

vibrational coordinate is expressed by creation and annihilation operators ($\mathbf{q} \propto [\mathbf{a}^+ + \mathbf{a}]$), and the light field (electric field vector \mathbf{E}) is written in terms of modes with frequencies ω_i (photon number density n_i in this mode) and the corresponding photon creation and annihilation operators ($\mathbf{E}_i \propto \omega_i^{1/2} [\mathbf{b}_i^+ + \mathbf{b}_i]$). If the molecular vibration is treated as a harmonic oscillator in a quantum state $|m\rangle$ and only the resonant mode of the infrared light field characterized by its photon number density (corresponding wave function $|n_{\text{IR}}\rangle$) is considered, the probability for a photon number change by ± 1 (according to the selection rules of a harmonic oscillator) is given by the difference of probabilities for emission and absorption of a photon (and decrease or increase of the oscillator quantum number by 1, respectively):

$$W_{\text{IR}} \propto |\langle n_{\text{IR}} + 1, m - 1 | \mathbf{b}_{\text{IR}}^+ \mathbf{a} | n_{\text{IR}}, m \rangle|^2 - |\langle n_{\text{IR}} - 1, m + 1 | \mathbf{b}_{\text{IR}} \mathbf{a}^+ | n_{\text{IR}}, m \rangle|^2 = (n_{\text{IR}} + 1)m - n_{\text{IR}}(m + 1) \quad (1)$$

This equation is now multiplied by total number of molecules N_{tot} , probability P_m for population of a vibrational state $|m\rangle$, and absorption/emission cross section σ_{IR} (a single σ_{IR} is used, because all vibrational states of a harmonic oscillator are equidistant, and line width and transition probability only depend on the quantum numbers of initial and final state¹⁰); taking then the sum over all vibrational states yields the rate of photon number change for a macroscopic number of molecules:

$$\frac{\partial n_{\text{IR}}}{\partial t} \propto \sigma_{\text{IR}} N_{\text{tot}} \sum_{m=0}^{\infty} P_m ((n_{\text{IR}} + 1)m - n_{\text{IR}}(m + 1)) = \sigma_{\text{IR}} N_{\text{tot}} \left(\sum_{m=0}^{\infty} (mP_m) - n_{\text{IR}} \right) \quad (2)$$

$\sum_{m=0}^{\infty} P_m = 1$ was used to derive the right side of eq 2. The first term contains information about the population of vibrational states, but does not depend on n_{IR} ; it describes IR fluorescence (spontaneous emission), which is normally too weak to be observed in condensed matter due to much more efficient nonradiative processes. If eq 2 is transformed to a

* Corresponding author. E-mail: g.seifert@physik.uni-halle.de. Fax: +49 345 5527221.

coordinate system moving with the velocity of light and then integrated, it is easily seen that the second term simply represents Beer's law, i.e., describes conventional absorption and stimulated emission. As this term is totally independent of the population distribution (and fluorescence is negligible), in the case of a harmonic oscillator no direct information about vibrational relaxation is accessible with infrared probing.

For Raman scattering processes the situation is different; two frequencies, namely these of incident probe ("laser", index L) and scattered light (Stokes: index S and anti-Stokes: index AS) have to be regarded, and the light fields must be written as sum of ($E_L + E_S$) or ($E_L + E_{AS}$). The probabilities for changes in n_S or n_{AS} are again given by the differences between emission and absorption probabilities:

$$W_S \propto |\langle n_L - 1, n_s + 1, m + 1 | \mathbf{b}_L \mathbf{b}_S^+ \mathbf{a}^+ | n_L, n_s, m \rangle|^2 - |\langle n_L + 1, n_s - 1, m - 1 | \mathbf{b}_L^+ \mathbf{b}_S \mathbf{a}^+ | n_L, n_s, n \rangle|^2 = n_L(n_s + 1) + n(n_L - n_s) \quad (3a)$$

$$W_{AS} \propto |\langle n_L - 1, n_{AS} + 1, m - 1 | \mathbf{b}_L \mathbf{b}_{AS}^+ \mathbf{a} | n_L, n_{AS}, m \rangle|^2 - |\langle n_L + 1, n_{AS} - 1, m + 1 | \mathbf{b}_L^+ \mathbf{b}_{AS} \mathbf{a}^+ | n_L, n_{AS}, m \rangle|^2 = n_{AS}(n_L + 1) - m(n_L - n_{AS}) \quad (3b)$$

In analogy to the case of a resonant IR light field (eq 2) molecular density, population probability and (scattering) cross sections σ_S and σ_{AS} for Stokes and anti-Stokes are introduced; the sum over all vibrational states gives the corresponding emission rates:

$$\frac{\partial n_S}{\partial t} \propto N_{\text{tot}} \sigma_S ((n_L - n_S) \sum_{m=0}^{\infty} (m P_m) + n_L (n_S + 1)) \quad (4a)$$

$$\frac{\partial n_{AS}}{\partial t} \propto N_{\text{tot}} \sigma_{AS} ((n_L - n_{AS}) \sum_{m=0}^{\infty} (m P_m) - n_{AS} (n_L + 1)) \quad (4b)$$

For the case of spontaneous Raman scattering, which is most important for studies of population relaxation processes, the number of scattered photons is very small, i.e., $n_S, n_{AS} \ll n_L$, and accordingly eqs 4 can be simplified to

$$\frac{\partial n_S}{\partial t} \propto N_{\text{tot}} \sigma_S n_L (1 + \sum_{m=0}^{\infty} (m P_m)) \quad (5a)$$

$$\frac{\partial n_{AS}}{\partial t} \propto N_{\text{tot}} \sigma_{AS} n_L \sum_{m=0}^{\infty} (m P_m) \quad (5b)$$

In contrast to the case of IR probing, both Stokes and anti-Stokes scattering contain population information even for harmonic oscillators. If only the ground state is populated (i.e., $P_{m=0} \neq 0, P_{m>0} = 0$), the sum in eqs 5 is zero, and thus only Stokes, but no anti-Stokes, photons will be observed. If also levels $m \geq 1$ are populated, the number of scattered Stokes photons increases due to the growing transition probability between higher levels (the probability of a $(m - 1) \rightarrow m$ transition is larger by a factor of m compared to the fundamental $0 \rightarrow 1$ transition); this increase is identical to the number of anti-Stokes photons (except the factor σ_S/σ_{AS}). But it is important to notice that only $m P_m$ can be obtained and not P_m alone. For example, one molecule in a $m = 2$ state cannot be distinguished from 2 molecules in the $m = 1$ state. The conclusion of the considerations so far is that in the idealized case of harmonic oscillators principally Raman scattering and IR fluorescence

would be suited for population relaxation studies; practically in liquids only Raman photons will be observable. But in any case only effective relaxation rates covering the manifold of overtones could be determined experimentally.

Turning to the more realistic case of a moderately anharmonic molecular vibration modified selection rules and energetic shifts of higher-lying levels must be regarded. But still transitions with $\Delta m = \pm 1$ are the strongest ones; only these will be discussed in the following. Now a $m \rightarrow (m + 1)$ or $(m + 1) \rightarrow m$ transition will be characterized by a central frequency ν_m , bandwidth Γ_m , and a frequency-dependent cross section $(m + 1)\sigma((\nu - \nu_m)/\Gamma_m)$, where the index m refers to the quantum number of the lower state of the considered transition. The prefactor $(m + 1)$ comes from the growing transition probabilities between higher levels (which are further described in harmonic approximation, which should be valid at least for moderate anharmonicities). As all these parameters are in general different for different transitions, the summation over all vibrational states cannot be simplified as much as for the derivation of eqs 2 and 5. If again IR fluorescence is neglected, the following expression is found instead of eq 2:

$$\frac{\partial n_{\text{IR}}}{\partial t} \propto N_{\text{tot}} n_{\text{IR}} \sum_{n=0}^{\infty} \left((m + 1) \sigma_{\text{IR}} \left(\frac{(\nu - \nu_m)}{\Gamma_m} \right) (P_{m+1} - P_m) \right) \quad (6)$$

Obviously for anharmonic oscillators also IR transmission can be modified by excess population if the transition frequencies for different m are sufficiently different. But at a distinct frequency ν_m always the population difference between the states $(m + 1)$ and m is probed. Only if there is no population in the upper level of the considered transition, population of a single (the lower) state can be determined separately. Experimentally, the relevant information, i.e., transient population changes $\Delta N(t) = N_{\text{tot}}(P_m - P_{m+1})$, is obtained calculating $\ln(T) - \ln(T_0) \propto \Delta N(t)$ (where T and T_0 denote sample transmission with and without previous excitation).

In a similar way, the spontaneous Raman scattering processes can be treated resulting in

$$\frac{\partial n_S}{\partial t} \propto N_{\text{tot}} n_L \sum_{n=0}^{\infty} \left((m + 1) \sigma_S \left(\frac{(\nu - (\nu_L - \nu_m))}{\Gamma_m} \right) P_m \right) \quad (7a)$$

$$\frac{\partial n_{AS}}{\partial t} \propto N_{\text{tot}} n_L \sum_{m=0}^{\infty} \left((m + 1) \sigma_{AS} \left(\frac{(\nu - (\nu_L + \nu_m))}{\Gamma_m} \right) P_{m+1} \right) \quad (7b)$$

It is easily seen looking at eqs 7 that changes of Raman scattering intensity at frequency shifts ($\nu_L \pm \nu_m$) only depend on single population probabilities, provided that the anharmonic frequency shifts ($\nu_{m+1} - \nu_m$) between different transitions are significantly larger than the corresponding line widths (Γ_m); in this case, population densities of single vibrational states can be determined. Interestingly the same excess population is seen at different frequency shifts; for example, the population of an $m = 1$ state can be measured on the anti-Stokes side at the (fundamental) frequency ν_0 or on the Stokes side at the (excited-state transition) frequency ν_1 . The ground state ($m = 0$) contributes only to Stokes, but not at all to anti-Stokes intensity. This difference has important consequences for experiments; while the number of scattered anti-Stokes photons is directly proportional to $\Delta N(t)$ and thus provides a "background-free" signal, in the Stokes case the same information is only found from differences of spectra with and without excess population, because there scattered intensity due to fundamental transitions

is much stronger than the changes to be observed. Another interesting point is that, if different normalization factors are not regarded, the difference between anti-Stokes and Stokes spectra is completely comparable to an IR spectrum (where, roughly spoken, the Stokes process corresponds to absorption, anti-Stokes to stimulated emission).

The discussion up to this point was only valid for oscillators with only one vibrational mode (two-atom molecules). For larger systems, all vibrations including their anharmonic coupling have to be taken into account. The principal contributions of this extension can be demonstrated introducing at least one additional vibrational state; that is, the wave function $|m\rangle$ has to be replaced by $|l,m\rangle$. Assuming that the field-matter interaction still only changes the quantum number m , eqs 6 and 7 remain valid if the single index m is replaced by a double index lm . Under these conditions a fundamental transition $|0,0\rangle \rightarrow |0,1\rangle$ can be distinguished from a $|1,0\rangle \rightarrow |1,1\rangle$ transition to a combination state if the corresponding line parameters (ν_{lm} , Γ_{lm}) for these two transitions differ. It is important to note that the level-dependent prefactor ($m + 1$) for these two transitions in harmonic approximation is equal (here, $=1$).

From the above considerations, it can be concluded that (i) successful studies of vibrational population dynamics in liquids are only possible if the investigated system is sufficiently anharmonic and (ii) it depends on selection rules (IR/Raman activity) for vibrational transitions if IR or Raman probing can provide the desired information. The amount of needed anharmonicity depends strongly on the spectral resolution of the experimental setup. The discussion will be continued in more detail after the Experimental Section.

Experimental Setup

The two laser systems used for the presented experiments are based on pulsed, Kerr-lens mode-locked Nd:YLF lasers with parametric frequency conversion stages; repetition rates are 70 or 60 Hz, respectively.

For the infrared double resonance system, pump and probe pulses are evaluated in two identical paths: First, a rather low percentage (2–3%) of an amplified single pulse is frequency-doubled (giving 523.5 nm); the second harmonic is then separated from the fundamental and sent through a KTP optical parametric generator (OPG); finally, the difference frequency between the idler from the OPG (1.2–2.0 μm) and the remaining fundamental is generated and amplified in, depending on wavelength range, LiNbO₃ or AgGaS₂ crystals. At the end of this procedure, two separately tunable pulses (tuning range 2.5–10 μm) with pulse durations of about 2.5 ps and a spectral width of 8–10 cm^{-1} are available; for the pump process up to 30 μJ of single pulse energy is produced, whereas in the probe beam the energy is diminished to $<1 \mu\text{J}$. For this investigation, only LiNbO₃ crystals were utilized. Transmission changes in a sample produced by (resonant) pumping are monitored by the probe pulses with time, frequency, and polarization resolution; a rotation-free signal ($\Delta\alpha_{\text{rf}}$), which is directly proportional to vibrational population changes can be obtained calculating $\Delta\alpha_{\text{rf}} = [\ln(T_{\parallel}/T_0) + 2 \ln(T_{\perp}/T_0)]/3$, where $T_{\parallel,\perp}/T_0$ denotes the parallel and perpendicular polarized component of measured sample transmission changes. The spectral resolution of this system is given by the spectral width of the infrared pulses. More details on this setup will be given elsewhere.¹¹

The system for observation of spontaneous Raman scattering after IR excitation comprises a pump path quite similar to that of the IRDRS system, but with an optical parametric oscillator (OPO) instead of the OPG; the probe pulse in this case is simply

provided by efficient second harmonic conversion of a single Nd:YLF pulse. The scattered Raman photons (the number of which is directly proportional to vibrational population) are collected and spectrally analyzed with a highly sensitive CCD camera behind a monochromator. Here, the spectral resolution depends on the grating used; for the experiments described below, a 384.7 lines/mm holographic grating was applied providing a spectral resolution of $\sim 13 \text{ cm}^{-1}$ ($\sim 23 \text{ cm}^{-1}$) at a Stokes (anti-Stokes) shift of 3000 cm^{-1} . This choice was the best compromise between spectral resolution and S/N ratio. For the data presented below, the Stokes spectrum for each delay position was collected two times, once with and once without IR excitation in order to have a reference spectrum under identical experimental conditions in each case. Details of this experimental setup have been described previously.¹²

To avoid stationary local temperature effects in the focal region precautions are taken to have a fresh portion of the (liquid) sample for each pump pulse: in the IRDRS system the sample cell is continuously moved within the focal plane by help of a motorized two-axes positioning stage, whereas in the Raman setup the interesting liquid is pumped through the capillary ($d = 200 \mu\text{m}$) of a specially designed IR quartz cell within a closed cycle.

Experimental Results and Discussion

This section has two aims: (i) the above theoretical considerations shall be illustrated and tested by experimental data and (ii) novel transient Stokes difference spectra will be introduced and compared to anti-Stokes and IR data from the same sample, and the additional information accessible from the Stokes data will be discussed. For this purpose, chloroform was re-examined, because this liquid provides sufficient IR and Raman activity at nearly all its fundamental vibrations, and its principal scheme of vibrational population relaxation has been cleared up in great detail in a previous study,¹³ where the transient population changes of all six fundamental vibrations could be traced using proper normalized time-resolved anti-Stokes spectra; the results are briefly summarized to facilitate the following discussion. It was found that the created transient population on the CH stretching level ν_1 has a lifetime of $\tau_1 = 23 \text{ ps}$, and the corresponding primary relaxation process is a three-quanta step, where one ν_1 vibrational quantum is converted into one ν_4 (CH bending mode) and one ν_2 (CCl₃ stretching vibration) quantum. It could not be determined if this means an intermolecular energy transfer (IET) process or intramolecular vibrational relaxation (IVR), i.e., transient population of a combination level like $\nu_2 + \nu_4$. Further findings were lifetimes of 105 ps for the ν_4 quanta, 460 ps for ν_2 quanta, energy redistribution between ν_2 and ν_5 on a time scale of 10 ps, and finally population of the low-lying levels ν_3 and ν_6 with a time constant of roughly 100 ps. The two limiting cases (IET or IVR) feasible for the description of the primary relaxation step are schematically given in Figure 1; levels ν_3 , ν_5 , and ν_6 are omitted for clearness. The dotted arrows symbolize transitions to over- or combination tones changing a ν_1 quantum; these “hot bands” are observable only in transient Stokes and IR spectra in accordance with the theoretical discussion. The corresponding frequency ranges (CH stretching region around $\sim 3000 \text{ cm}^{-1}$) of novel time-resolved Stokes difference spectra and transient IR transmission changes measured on neat chloroform at room temperature are plotted as three-dimensional surfaces in Figure 2; the CH-stretching mode ν_1 at 3020 cm^{-1} was excited. Figure 2a gives the relative (rotation-free) IR transmission changes $\ln(T_0/T)$, and Figure 2b gives the difference of scattered Stokes intensities with and

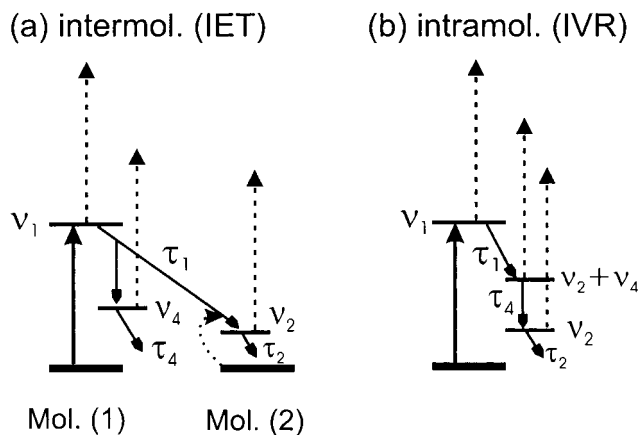


Figure 1. Simplified energy level schemes describing the vibrational relaxation of chloroform after CH stretch excitation for two limiting cases: (a) the first relaxation step being purely intermolecular and (b) relaxation being completely intramolecular.

without previous IR excitation of the CH stretch, in both cases as a function of delay time and frequency (shift). Both surfaces are created directly by connecting experimental data points linearly. It is easily seen that the time and frequency dependence of the two signals are quite similar, with only one striking difference: in the IR data, a much more pronounced negative peak at $t_{\text{del}} = 0$ ps and $\nu_{\text{pr}} = 3020$ cm^{-1} is observed. Looking in more detail, in both cases three common characteristic features are observed, which can easily be interpreted regarding the outcome of the mentioned anti-Stokes investigation¹³ and similar experiments on bromoform.¹⁴ (i) At the fundamental frequency (3020 cm^{-1}), the signals decrease very fast to a minimum near delay zero, then more slowly increase again, though staying clearly below their equilibrium values even 300 ps after the excitation process; this first feature is directly proportional to ground state depletion in the Stokes case, whereas in the IR spectra additionally stimulated emission contributes to the observed change. It should be noted that this fully corresponds to the theoretical considerations. (ii) At ~ 2900 cm^{-1} , the observed scattering intensity (or absorption increase, respectively) increases steeply to a maximum near $t_{\text{del}} = 0$ ps and then returns to its equilibrium value within less than 100 ps; this signal is due to excited state absorption ($v = 1 \rightarrow v = 2$ transition of the CH stretch) confirming both the ν_1 lifetime of 23 ps and the anharmonic shift of 125 cm^{-1} for the first CH stretch overtone obtained from conventional IR spectra. (iii) Around 2995 cm^{-1} , there is a moderately slow increase of the signal to a maximum at $t_{\text{del}} = 50$ ps, followed by a quite slow decay; this feature is caused by transitions starting from lower-lying levels (which are populated in the course of ν_1 relaxation) and ending at the corresponding combination state with ν_1 . This type of transition was discussed at the end of the theoretical section.

For the transient spectra at zero delay, i.e., maximum ν_1 population, the validity of the theoretical prediction of transition probabilities in the harmonic oscillator limit can be tested. The $1 \rightarrow 2$ transition is expected to have two times the band integral of the $0 \rightarrow 1$ transition; this ratio should be found in the Stokes spectra comparing features (i) and (ii), while in the IR case the additional stimulated emission should lead to equal band areas (denoted by Δ in the following). Calculating the band integrals Δ_{01} and Δ_{12} at $t_{\text{del}} = 0$ directly from the data yields ratios of $\Delta_{12}/\Delta_{01} = 2.0$ for the Stokes intensity change and $\Delta_{12}/\Delta_{01} = 1.13$ for the IR transmission changes. This agrees, within experimental accuracy, quite well with the expectation; it can be concluded that the use of amplitude arguments derived from

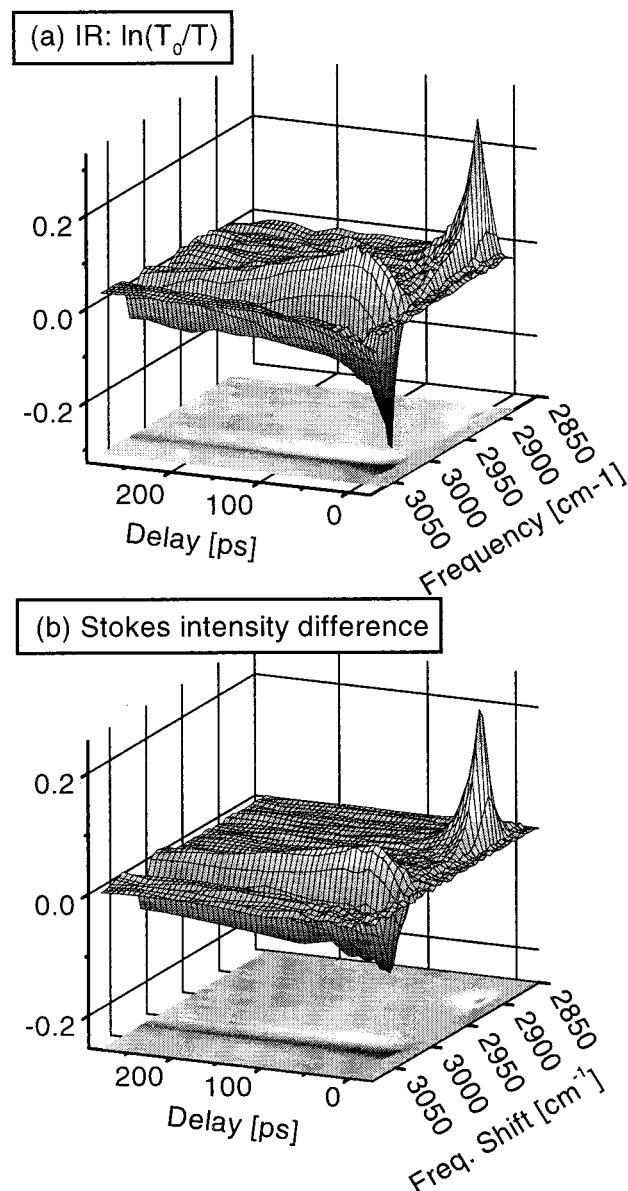


Figure 2. 3D surface plots of measured transient spectral changes in the CH stretching region of liquid chloroform as a function of delay between pump (at 3020 cm^{-1}) and probe pulses: (a) ratio of IR transmission $\ln(T_0/T)$ without and with excitation; (b) difference of Stokes intensities with and without IR excitation.

the harmonic oscillator model is well justified for the presented data despite the rather large anharmonic shift of the $1 \rightarrow 2$ transition.

One can now try to extend these amplitude arguments for the Raman Stokes scattering to distinguish between the IVR and IET relaxation processes as depicted in Figure 1. As just discussed, the expectation of a normalized integrated Stokes intensity of 1 around 3020 cm^{-1} (fundamental transition) and 2 around 2900 cm^{-1} (excited state transition) at early delay times is approximately confirmed by the data. At later times, the situation of Figure 1a would mean two lacking ground state molecules (transitions) and two combination transitions for each primarily excited molecule, resulting in a band area of 2 both for the depleted fundamental and additional combination tone scattering. In the situation of Figure 1b, these two band areas would be 1. In consequence, a careful comparison of short and long time behavior should allow a decision between the two situations. Unfortunately, in the case of chloroform, the various

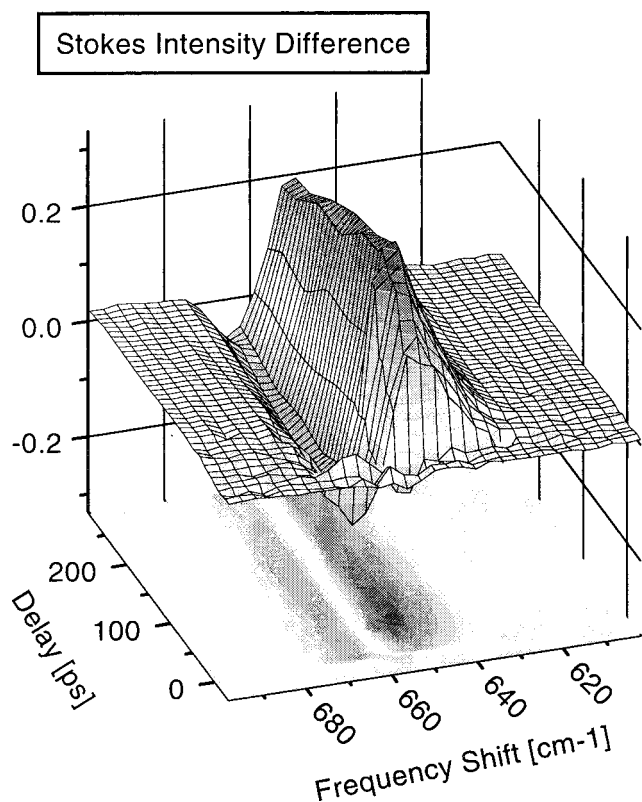


Figure 3. 3D surface plot of measured transient Stokes intensity differences in the ν_2 (symmetric CCl_3 stretching) region of liquid chloroform as a function of delay between pump (at 3020 cm^{-1}) and probe pulses.

overlapping transitions to combination levels (which are responsible for the induced absorption around 2995 cm^{-1}) make it impossible to derive the desired information. In the appropriate frequency region the following transitions have to be considered: $\nu_4 \rightarrow (\nu_1 + \nu_4)$ with anharmonic shift of 22 cm^{-1} ; $\nu_2 \rightarrow (\nu_1 + \nu_2)$ and $\nu_5 \rightarrow (\nu_1 + \nu_5)$, both with $\sim 4\text{ cm}^{-1}$ shift; $\nu_3 \rightarrow (\nu_1 + \nu_3)$ and $\nu_6 \rightarrow (\nu_1 + \nu_6)$, shifts $\leq 2\text{ cm}^{-1}$; $(\nu_2 + \nu_4) \rightarrow (\nu_1 + \nu_2 + \nu_4)$, where the anharmonicity cannot be determined directly from overtone spectra, but estimated to be $< 25\text{ cm}^{-1}$ from the above numbers. As the anharmonic shifts are in most cases clearly smaller than the spectral width of the CH stretching band, positive and negative contributions compensate each other to a large extent. A simulation using the two limiting relaxation models of Figure 1 and three Lorentzian lines with realistic anharmonic shifts revealed that the amplitudes of the expected spectral features for inter- and intramolecular case, respectively, only differ by less than 15% instead of the factor of 2 expected for isolated bands. Accordingly, within experimental accuracy the in principle available information if IET or IVR is dominating cannot be extracted from the data in the CH stretching region.

But of course, the Stokes spectra were recorded in the whole accessible frequency range, thus particularly also at low-lying fundamentals (which cannot be monitored with our current IR setup and are in general hard to measure using IR pulses). As an example, the region around the ν_2 band (at 665 cm^{-1}) is presented in Figure 3, again as a three-dimensional surface plot. Only two effects are seen: (i) at the fundamental frequency the scattered intensity decreases rapidly due to ground state depletion, then remains constant or even decreases slightly more up to $\sim 100\text{ ps}$, and afterward begins to increase again; (ii) at a red-shift of $\sim 13\text{ cm}^{-1}$, the intensity increases more slowly to a significantly stronger maximum around 70 ps and then decreases

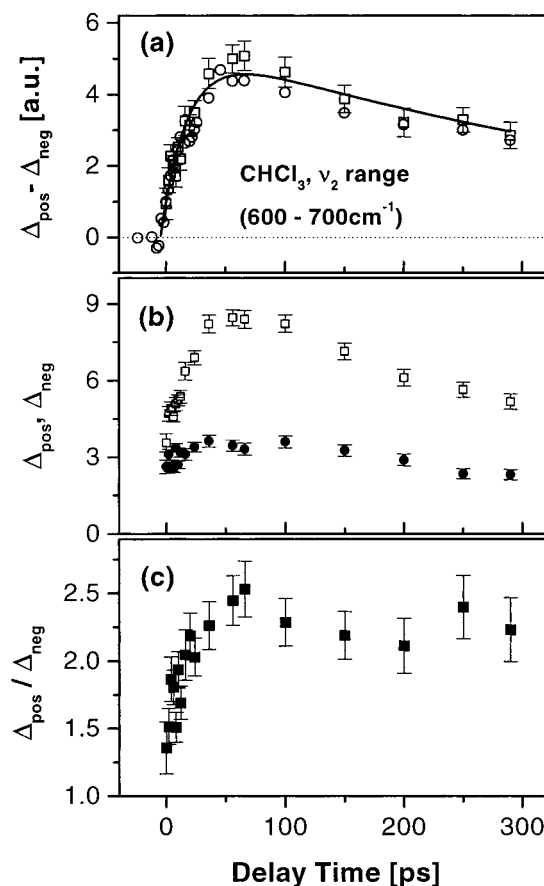


Figure 4. Integrated band areas calculated from the ν_2 region of transient Stokes difference spectra of chloroform: (a) direct integration (circles) and sum of two Lorentzian lines (squares, see (b)); (b) areas of two Lorentzian bands fit to the ν_2 region, (open squares) positive contribution, (solid circles) negative contribution; (c) ratio $\Delta_{\text{pos}}/\Delta_{\text{neg}}$ of the bands given in (b).

quite slowly. Again, a detailed analysis of the observed features suffers a little from the overlap of positive and negative effects, but nevertheless in this spectral region important additional information can be obtained from an evaluation of the data; the results are presented in Figure 4.

First of all, the whole spectral range presented in Figure 3 can be integrated (Figure 4a, open circles) giving the changes of population probabilities times quantum numbers ($\sum \Delta(mP_m)$; compare eq 5a). It is obvious that the population of the ν_2 manifold increases. This observation is in very good agreement with the anti-Stokes results for the ν_2 band,¹³ where the time evolution of its transient population could be described by the proportionality $\Delta n_2(t) \propto (\exp(-t/\tau_{\text{eff}}) - \exp(-t/\tau_1))$ with $\tau_{\text{eff}} = 460\text{ ps}$ and $\tau_1 = 23\text{ ps}$; using the same expression and exactly the same time constants the solid curve in Figure 4 was calculated (with an amplitude factor of 5.6). The better frequency resolution of the presented Stokes data allows a more detailed analysis: if higher levels ($m \geq 1$) of the ν_2 manifold are populated, one expects regarding eq 7a that the negative component mainly belongs to the lacking ground state molecules, whereas the positive (red-shifted) contribution is due to the population of the higher levels.

Fitting the transient Stokes intensity differences by two Lorentzian lines, the band areas given in Figure 4b as full circles (Δ_{neg}) and open squares (Δ_{pos}) were found (frequency and width of the negative line, i.e., the lacking fundamental were fixed). The difference of these areas (shown in Figure 4a as open

squares) nicely agrees with the direct integration result. Finally, the quotient of the band areas is shown in Figure 4c.

The time dependence of the positive band alone is rather similar to the integrated band intensity; the slight differences can readily be explained by contributions of transitions such as $\nu_1 \rightarrow (\nu_1 + \nu_2)$ and $\nu_4 \rightarrow (\nu_4 + \nu_2)$. More interesting is the behavior of the negative band; in the limit of pure intramolecular relaxation, the maximum ground state depletion would be reached at the end of the pump process, i.e., after ~ 5 ps, and from then on could only decrease. In contrast to this, the solid points in Figure 4b indicate that in chloroform ground state depletion is at least constant up to 100 ps or even increases slightly up to this point of time. This cannot be explained by population of ν_2 from the thermal bath (due to already relaxed energy) because this process is expected to occur with a time constant slower by a Boltzmann factor (here, 5 with respect to ν_3 and ~ 25 with respect to ground state) compared to the lifetime of 460 ps; this means, direct thermal population can only happen on a nanosecond time scale and should thus be negligible within the first 100 ps. Accordingly, this observation is a significant hint that in liquid chloroform there is a certain amount of intermolecular interactions increasing the number of vibrationally excited molecules within the first 100 ps after excitation. The magnitude of this increase can be estimated to be of the order of 20%. Another piece of information can be obtained by looking at Figure 4c. On the basis of eq 7a one would expect the intensity ratio $\Delta_{\text{neg}}/\Delta_{\text{pos}}$ to increase from 1 at early times (population of ν_1) to a larger value at later times due to population of ν_2 modes; particularly, if any molecule which is not in the ground state would contain one ν_2 quantum, a ratio of 2 should be found. The observed value at longer times is slightly higher; this can either be interpreted as contribution of $2\nu_2$ population or by a rather strong anharmonic increase of the transition probability compared to the harmonic approximation.

Finally, it must be discussed why the increase of ground state depletion was not observed in the CH stretching region. A possible explanation is found looking at the quite different ratios of anharmonicity and bandwidth in the two spectral regions. While, e.g., the transition $\nu_2 \rightarrow (\nu_1 + \nu_2)$ exhibits an anharmonic shift of 4 cm^{-1} with a ν_1 bandwidth of $\sim 14 \text{ cm}^{-1}$, the $\nu_2 \rightarrow 2\nu_2$ band is red-shifted by $\sim 7 \text{ cm}^{-1}$ and the ν_2 bandwidth is $\sim 9 \text{ cm}^{-1}$; similar numbers are found for other transitions. So it seems plausible that in the CH region ground state depletion and population of low-lying levels nearly perfectly compensate each other, while they are well separable in the case of the CCl_3 stretching mode ν_2 . More details could be obtained analyzing further spectral regions and/or data with higher spectral resolution, but this would go beyond the aim of this work.

Conclusion

The following conclusions can be drawn summarizing the above theoretical considerations and the presented analysis of experimental data on chloroform. First of all, studies of transient vibrational population require anharmonic frequency shifts larger than the applied spectral resolution. In the case of a moderately anharmonic vibrational system (like the presented liquid chloroform), on one hand it becomes possible to trace transient populations of single vibrational levels by both IR and Raman probing, on the other hand the harmonic approximation for the ratios of transition probabilities may still be used in the data analysis.

Transient Stokes difference spectra open up the possibility to study not only population on all Raman active vibrations (like in the case of anti-Stokes) but additionally also ground state depletion in the region of any fundamental. In particular, a spectral region with sufficient anharmonic shifts can be selected in order to work on the question of inter- or intramolecular energy transfer in the course of vibrational relaxation; this kind of analysis could be demonstrated for the presented results in the CCl_3 stretching region ($600\text{--}700 \text{ cm}^{-1}$) with the outcome that in liquid chloroform obviously an intermolecular energy transfer is present within the first 100 ps, but intramolecular processes are dominating the relaxation. The great similarity of transient Stokes difference spectra and IR transmission changes, which roughly spoken differ just by the corresponding anti-Stokes photons, could be demonstrated on the same sample.

Taking a quite general, but experimental, point of view, Raman probing of vibrational excess population is favorable for studies of corresponding ultrafast dynamics, because there is no need for tunability of the probe light and the comprehensive information can in principle be obtained from a single experiment. Even for low-lying levels the signal can be detected in the visible, where in contrast to far-IR, highly sensitive detectors are available. On the other hand, there are vibrational modes with very low Raman cross section, where often the signal cannot be distinguished from noise. As this is the case particularly in the presence of hydrogen bonds, there is still a wide range of interesting investigations, where IR probing is the better (if not the only) choice. And, applying complete polarization resolution, not only information on orientational relaxation but also about the real part of $\chi^{(3)}$ can be obtained simultaneously from the IR experiment. So in general, the two probe techniques complement each other quite nicely, and a combination of both, particularly if both anti-Stokes and Stokes scattering is analyzed, is a very efficient method to obtain real comprehensive information about the equilibration of vibrational excess energy.

References and Notes

- (1) Laubereau, A.; Kaiser, W. *Rev. Mod. Phys.* **1978**, *50*, 697.
- (2) Heilweil, E. J.; Casassa, M. P.; Cavanagh, R. R.; Stephenson, J. C. *J. Chem. Phys.* **1984**, *81*, 2856.
- (3) Graener, H.; Dohlus, R.; Laubereau, A. *Chem. Phys. Lett.* **1987**, *140*, 306.
- (4) Bakker, H. J. *J. Chem. Phys.* **1993**, *98*, 8496.
- (5) Seifert, G.; Graener, H.; Laubereau, A. *Chem. Phys. Lett.* **1990**, *172*, 435.
- (6) Graener, H.; Ye, T.-Q.; Laubereau, A. *J. Chem. Phys.* **1989**, *90*, 3413. Graener, H.; Seifert, G.; Laubereau, A. *Phys. Rev. Lett.* **1991**, *66*, 2092.
- (7) Laenen, R.; Rauscher, C.; Laubereau, A. *Phys. Rev. Lett.* **1998**, *80*, 2622. Seifert, G.; Graener, H. *J. Phys. Chem.* **1994**, *98*, 11827.
- (8) Flynn, G. W. In *Chemical and biological applications of lasers*; Moore, C. B., Ed.; Academic Press: New York, 1974. Yardley, J. T.; Moore, C. B. *J. Chem. Phys.* **1968**, *49*, 1111.
- (9) Seifert, G.; Hofmann, M.; Weidlich, K.; Graener, H. In *Proceedings of Ultrafast elementary processes in chemical and biological systems*; AIP Conference Proceedings 364; American Institute of Physics: Woodbury, NY, 1996; pp 131–138.
- (10) Fischer, S. F.; Laubereau, A. *Chem. Phys. Lett.* **1975**, *35*, 6. Madden, P. A.; Lynden-Bell, R. M. *Chem. Phys. Lett.* **1976**, *38*, 163.
- (11) Seifert, G.; Graener, H. To be published.
- (12) Hofmann, M.; Graener, H. *Chem. Phys.* **1996**, *206*, 129.
- (13) Graener, H.; Zürl, R.; Hofmann, M. *J. Phys. Chem. B* **1997**, *101*, 1745.
- (14) Graener, H. *Chem. Phys. Lett.* **1990**, *165*, 110.